ROYAL SOCIETY OF CHEMISTRY

PAPER

Check for updates

Evaluating the accuracy of two *in situ* optical sensors to estimate DOC concentrations for drinking water production†

S. Hoffmeister, [iD] *[ab] K. R. Murphy,[c] C. Cascone, [iD] [a]
J. L. J. Ledesma [iD] [ad] and S. J. Köhler[a]

Two *in situ* optical sensors, a single-excitation fluorescence-based sensor (fDOM) mounted on a multi-parameter EXO2 sonde (YSI), and a stand-alone, multispectral absorbance-based instrument (spectro::lyser, scan Messtechnik GmbH), were evaluated for their capability to (i) estimate river dissolved organic carbon (DOC) concentrations and (ii) provide oversight of drinking water production. The sensors were deployed between March and November 2017 in the river Fyris, which drains a mixed forested and agricultural 2003 km^2 catchment and serves as a drinking water source by managed aquifer recharge. Grab samples were collected every 2 to 3 weeks and compared with logged sensor data collected at 15 minute intervals. The fDOM probe signal was used to estimate DOC concentrations in the range of 10.4 to 24.4 mg L^{-1} using linear regression (R^2 = 0.71, RMSE = 2.5 mg L^{-1}), after correction for temperature, turbidity and inner-filter effects. Temporal changes in DOC character associated with the mixed land use landscape, as indicated by optical indices, reduced this sensor accuracy for estimating DOC concentration. Nevertheless, humic substance concentrations, the fraction of DOC that is preferentially removed during artificial infiltration, were well captured. The spectrolyser signal was used to establish a 2-component partial least square model that captured DOC fluctuations from 10.2 to 29.4 mg L^{-1} (R^2 = 0.92; RMSE = 1.3 mg L^{-1}). This multiple-wavelength model (220 to 720 nm) effectively handled the changes in DOC composition while accurately estimating DOC concentrations. This study explores the advantages and limitations of optical sensors for their use in managed aquifer recharge and drinking water production in relation to DOC levels.

Water impact

Tracking fast and unpredictable changes in source water quality is crucial for optimized drinking water production. Current increased development of *in situ* water quality sensors can help anticipate those changes, but their implementation is still constrained by uncertainties. Studies comparing different sensor techniques are often conducted in the laboratory. Here we examine the application of two different sensors under field conditions.

1. Introduction

Northern Europe experienced an extremely dry summer in 2018, which highlighted the vulnerability of drinking water supplies and the challenges of suppliers in the face of a changing climate.[1] Expected changes in meteorological

[a] Department of Aquatic Sciences and Assessment, Swedish University of Agricultural Sciences (SLU), Lennart Hjelms väg 9, 75007 Uppsala, Sweden
[b] Karlsruhe Institute of Technology (KIT), Institute of Water and River Basin Management, Chair of Hydrology, Kaiserstraße 12, 76131 Karlsruhe, Germany. E-mail: svenja.hoffmeister@kit.edu
[c] Chalmers University of Technology, Architecture and Civil Engineering, Water Environment Technology, Sven Hultins Gata 6, 41296 Gothenburg, Sweden
[d] Centre for Advanced Studies of Blanes, Spanish National Research Council (CEAB-CSIC), Accés a la Cala Sant Francesc 14, 17300 Blanes, Spain
† Electronic supplementary information (ESI) available. See DOI: 10.1039/d0ew00150c

conditions (*e.g.* heat waves, sudden heavy precipitation events) will lead to greater variation in the quantity and quality of surface waters, which are used by 50% of Nordic drinking water producers.[2] Due to this, and decreased acid deposition, surface waters are experiencing "browning" which manifests as increased dissolved organic carbon (DOC) concentrations and associated yellow to brown colour.[3–5] DOC is of concern to drinking water producers as it is linked to unwanted colour, taste, odour and risk of (i) bacterial growth in the distribution network, (ii) membrane fouling, and (iii) disinfection by-products posing potential health threats.[6–9] In combination with greater water demand due to a growing population and expanding cities, browner water requires more costly treatment, potentially including higher coagulant doses,[10] retrofitted treatment steps,[11] and improved pre-treatment.

In Sweden and other Scandinavian countries, artificial infiltration of surface water through managed aquifer recharge (MAR) is often employed as an efficient pre-treatment process[12] that can help to smooth out fluctuations in raw water quality and quantity. Additional benefits include low and stable temperature and natural removal of colour, pathogens, nutrients and metals, reducing the need for posterior treatment inside drinking water facilities. However, large fluctuations in infiltration water quality can threaten proper MAR functionality. High DOC concentrations in the source water could exceed the natural removal capacity and lead to clogging issues, disrupting the process and reducing overall water quality.[13] Hence, monitoring of DOC concentrations becomes necessary to adjust infiltration fluxes accordingly and to minimize risks and costs.

Fluorescence and absorbance spectroscopy have been used in a large number of studies to track water quality changes, mainly related to changes in DOC character.[14–19] Analysing fluorescence excitation-emission matrices (EEM) is a very powerful tool to quantify subtle changes in DOC character[15,20–22] that may correlate to macroscopic parameters such as molecular weight,[23] but EEMs are data-intensive. Optical indices can also be useful tools to understand DOC dynamics[24] and some can be rapidly obtained with online sensors that measure only restricted wavelengths. Specific ultra violet absorbance (SUVA) is widely used in the drinking water sector to predict the presence of hydrophobic substances.[19] Humic substances (HS), detected by e.g. liquid chromatography-organic carbon detection LC-OCD,[25] are a fraction of DOC that are well-removed during coagulation treatment.[19,26–29] SUVA and HS/DOC are reportedly good indicators of treatability.[27]

DOC concentrations and character vary on a range of timescales, including seasonal, daily, and sub-daily through changing source areas and in-stream processes.[30] High-frequency sensors can record rapid changes in water quality that might be missed by a program involving only intermittent (grab) sampling. Collecting real-time high-frequency measurements based on absorbance or fluorescence of the ingoing raw water will increase the efficiency of MAR management processes by allowing an immediate response to peaks in turbidity and DOC concentrations, which includes shutting down the MAR to protect the aquifer much earlier than what is the case today.

Due to differences in technical functioning and sensitivity, it is presently unclear whether fluorescence- and absorbance-based sensors provide comparable water quality information, and whether they are worth incorporating into a MAR management scheme. Optical measurements are influenced by the sample matrix, and corrections for temperature quenching, turbidity and inner-filter effects (IFE) need to be performed prior to analysis of the data.[31–36] In this study, we evaluated whether two optical sensors (one fluorescence-based and one absorbance-based) can provide accurate DOC concentration estimates and beneficial additional information for drinking water production compared to intermittent grab samples. Specifically, we aimed to answer two questions: 1) how accurate are the two different optical sensors in estimating DOC concentrations, and 2) how useful is their application for drinking water production. Additionally, we investigated DOC and catchment dynamic-related processes from the knowledge gained during the measurement period from the combination of sensors and grab samples.

2. Material and methods

2.1. Site description

The river Fyris, hereafter Fyrisån, is the main raw water source for two drinking water treatment plants servicing the population of Uppsala, Sweden. It flows along 80 km from North to South (Fig. 1) and discharges into lake Ekoln, which is part of lake Mälaren (Sweden's third largest lake with 1090 km^2), draining into the Baltic sea. The annual specific discharge is 204 ± 63 mm per year (1995–2010).[37] Fyrisån is typically dominated by low runoff during summer and high runoff during autumn (a consequence of autumn rainfalls and reduced evapotranspiration) and spring (a consequence of snowmelt).[38] It is one of the largest contributors of DOC per unit of area of all Mälaren tributaries, with an average load of 3.3 ± 1.3 g C m^{-2} per year (1995 to 2010).[37]

The Fyrisån catchment covers 2003 km^2 with elevations ranging from 15 to 115 $m^{37,39}$ and is mostly covered by forest (63%, mostly coniferous trees), followed by agricultural lands (32%). Urban areas make up about 3% and wetlands/lakes add up to about 2%. Precipitation is on average 557 ± 87 mm per year (1981–2010) and the mean annual temperature is 6.1 ± 1.0 °C (1981–2010). When the river water level falls below a threshold, water from the adjacent lake Tämnaren and river Vendelån (each contributing with about 0.6–0.7 m^3 s^{-1}) is pumped into the river to maintain a minimum water level. The main study site, Storvad, is located ca. 12 km upstream of the city Uppsala, and about 19 km from the river outlet (Fig. 1). At this location the river water is most representative for the raw water inside the drinking water treatment plant.

2.2. Grab sampling and laboratory measurements

In total, 19 grab samples were collected at the Storvad site between March and November 2017 with an interval of 2 to 3 weeks. Filtered samples (pre-burned GFF, nominally 0.7 μm) were analysed for absorbance, fluorescence and DOC concentration in the laboratory. Measurements of absorbance spectra and fluorescence EEMs were performed with an Aqualog (Horiba Jobin Yvon) and a 1 cm quartz cuvette (excitation wavelength range: 250 to 450 nm, emission 212 to 620 nm, at 2 nm intervals).[40] The EEMs were corrected within the associated Aqualog® software FluorEscence™ for IFE of the EEMs using the EEM of Milli-Q and Rayleigh masking to remove primary and secondary Rayleigh peaks. Intensities were converted to Raman units (RU) by dividing the measured fluorescence by the Raman peak area of pure water.[41] In the
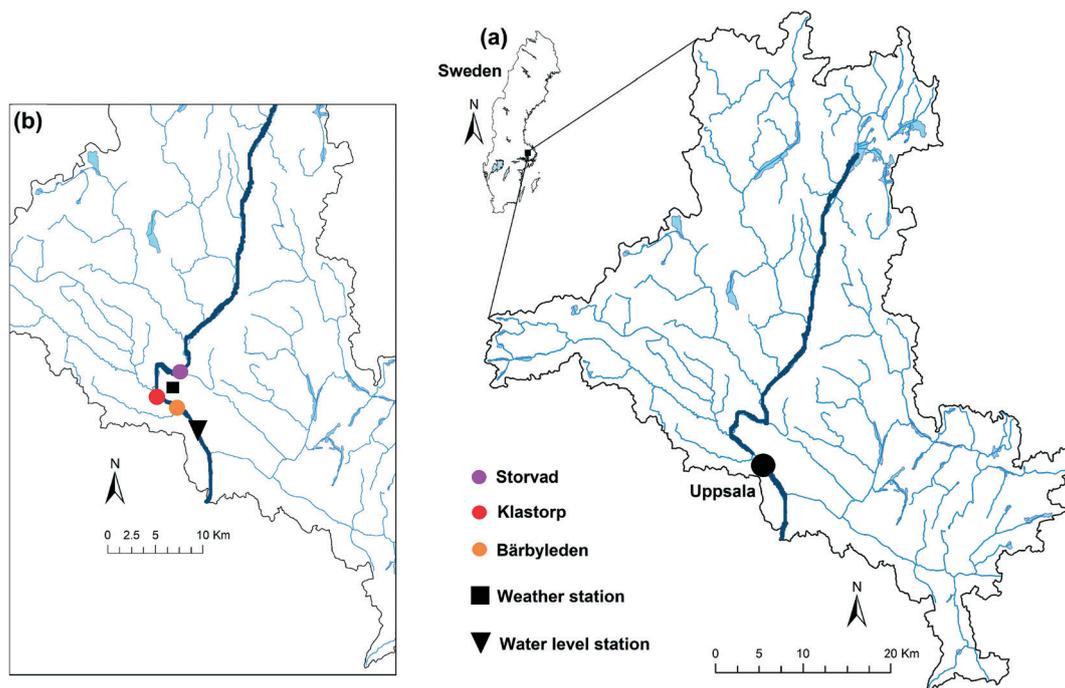
Fig. 1 Map of the Fyrisån catchment in Southeast Sweden (a). The inset (b) shows the locations of the sampling sites as well as weather and water level stations.

following, the term "corrected" EEMs refers to the EEMs treated following this procedure. For comparison of laboratory data with *in situ* measurements, the RU units were converted to QSU by simple linear regression. DOC concentration was measured using a Shimadzu TOC-VCPH carbon analyser by catalytic combustion with a precision of about 0.2 mg L^{-1}. For quality assurance, standards and Milli-Q water were measured with each batch of samples (absorbance: K-phthalate (10 mg L^{-1}), DOC: EDTA 10 ± 0.15 mg L^{-1}).

2.3. *In situ* measurements (fluorescence and absorbance sensors)

A fluorescence-based sensor tracking fluorescent dissolved organic matter, fDOM on EXO2 (YSI),[42] and an absorbance-based sensor, s::can spectro::lyser (scan Messtechnik GmbH),[43] were programmed to record data at 15 min intervals. The sensors were deployed inside the pumping station at Storvad which provided electricity and protection from external threats (*e.g.* weathering, vandalism). River water, pumped into the pumping station, passed through the measuring path of the spectrolyser before draining into an overflow bucket, into which the EXO2 was immersed (Fig. A1, ESI†).

2.3.1. fDOM sensor. The EXO2 probe is a battery-supplied multi-parameter 6-port device with anti-fouling wiper. The device used here was equipped with sensors that measure pH, conductivity/temperature (T_{meas}), turbidity ($Turb_{meas}$) and fDOM ($fDOM_{meas}$). Additionally, a wiper was installed centrally to wipe the sensors before each measurement. Calibrations were performed according to the manufacturer

manual guidelines.[42] The fDOM sensor is an optical fluorescence sensor with an excitation wavelength at 365 ± 5 nm, and emission wavelength at 480 ± 40 nm. A two-point calibration was performed, using pure water (*i.e.* 0 µg C L^{-1}) as the first calibration standard, and a 300 µg C L^{-1} quinine sulphate solution as the second standard, to produce data in quinine sulphate equivalent units (QSU).

2.3.2. Absorbance sensor. The spectrolyser measured absorbance spectra ranging from 220 to 720 nm at 2.5 nm intervals and had a path length of 0.5 cm. Automatic cleaning was conducted twice per day by pressurized air supplied from an oil-free compressor. Manual cleaning with a smooth brush and lint-free cloths took place when collecting grab samples. Connection to the mains was required both for the compressor and the device itself.

2.4. Calibration datasets

Field experiments were undertaken for *in situ* calibration of turbidity, absorbance and temperature effects on fDOM prior to deployment. To acquire correction functions valid for a wide range of measurements, data of higher and lower concentrations than the expected measured time series had to be generated. Both sensors were placed into a shallower part of the river (*ca.* 30 cm) around 19 km downstream of the main study site at a nearly-constant temperature of about 10 °C. After a five minute period for adaptation and recording of stable data, turbidity was increased by manually stirring the water and thereby dispersing the sediment near the sensor. The stirring was stopped after five minutes and data logging

continued until turbidity decreased to approximately pre-experiment conditions. As the calibration data set was recorded in less than an hour under calm weather conditions, DOC concentrations were assumed to be stable (11.4 ± 0.1 mg L^{-1}) and all observed changes of $fDOM_{meas}$ were assigned to the introduced variations of turbidity from manual stirring thus facilitating the calibration procedure. During these experiments, data were recorded every 30 seconds by the EXO2 and every minute by the spectrolyser. A grab sample was taken adjacent to the sensors for laboratory analyses of filtered aliquots for DOC, absorbance and fluorescence using the Aqualog. The EXO2 device was exposed to the same water sample after overnight storage in a cooling room (6 °C) for measurements at low temperatures. The lab experiments for calibrating the temperature dependency of the optical sensors were undertaken at a fixed DOC concentration (11.4 mg L^{-1}).

Dilution experiments were used to investigate concentration-related biases in the *in situ* fDOM signal and to develop a correction function for the field measurements. For this, a river sample with known DOC concentration (26 mg L^{-1}) was diluted five times in series to obtain samples with the same organic matter composition but with different DOC concentrations and absorbance. For each dilution, fDOM was measured with the sensor attached to the EXO2 and absorbance and DOC were analysed in the laboratory.

2.5. Supplementary catchment data

One site within the Fyrisån catchment (Klastorp, Fig. 1) has been sampled monthly as part of the long-term Swedish environmental monitoring program.[44] Due to its relatively close positioning to the Storvad study site (*ca.* 7 km downstream), Klastorp data were used to complement the study dataset. Analogously to the samples from Storvad, samples from Klastorp were analysed in the laboratory for absorbance, fluorescence and DOC concentration, and additionally as a routine of the monitoring program among others for silica and filtered iron concentrations and absorbance at 420 nm (Abs_{420}) (Fig. A2, ESI†). Furthermore, data from another EXO2 sensor 9 km downstream of Storvad

(Bärbyleden, Fig. 1) were available for comparison for part of the study period, producing overlapping sensor data series (data not shown). Water level data were obtained from Uppsala University from a pressure transducer installed in the city centre, approximately 14 km downstream of the study site. Hourly discharge was calculated based on an existing rating curve for this river section.

2.6. Data treatment

2.6.1. Laboratory fluorescence metrics. For each of the grab samples analysed in the laboratory, three optical indices were calculated from the corrected EEMs: humification index (HIX),[45] fluorescence index (FI)[46] and freshness index ($\beta : \alpha$).[47] Definitions and interpretations of these indices are presented in Table 1. Additionally, intensities of T and C peaks were located in the EEMs and the resultant ratio of T/C calculated.[48] The T/C peak region is sensitive to changes in the DOC character and can thus provide important information for understanding both the DOC quality and the sensor's response.

2.6.2. Laboratory absorbance metrics. SUVA values were calculated from absorbance measurements at 254 nm (Abs_{254} [cm^{-1}]) and DOC concentrations. Abs_{254} was utilized to approximate concentrations of HS [mg L^{-1}]. The equation is based on LC-OCD measurements sampled in both Fyrisån and along the infiltration area.[49]

$$HS = 1.1 + 19.2 \, Abs_{254} \tag{1}$$

2.6.3. *In situ* fluorescence (fDOM) corrections and DOC estimation. The EXO2 fDOM sensor measures at similar wavelengths as the defined peak C (*i.e.* excitation: 365 ± 5 nm, emission: 480 ± 40 nm) and hence captures the humic-like peak (Table 1). Fluctuations in turbidity and temperature interfere with the fluorescence sensor signal. Thus, the $fDOM_{meas}$ signal from the EXO2 sensor was corrected for the effects of turbidity, temperature and IFE using a modified version of the method presented by Downing *et al.*[32]

Instrument-specific functions for the correction of turbidity and IFE were obtained by using the calibration

Table 1 Definition and interpretation of established optical indices used in this study. A = area under the curve. Em = emission. Ex = excitation. Numbers refer to wavelength [in nm] unless otherwise specified. References provided in the text

Index	Definition [No. in nm (if not other indicated)]	Interpretation
HIX	Em: $A(345 - 480)/[A(300 - 345) + A(435 - 480)]$ Ex: 254	Degree of humification; high HIX = more humified material
FI	Em: 470/520 Ex: 370	Source; gradient from higher FI (more microbial) to smaller FI (more terrestrial)
$\beta : \alpha$	Em: 380/max(420–435) Ex: 310	Age; higher $\beta : \alpha$ = larger contribution of more freshly produced DOC
Peak T	Em: 275 Ex: 340	Tryptophan-like peak
Peak C	Em: 450 Ex: 350	Humic-like peak
T/C	Intensity (peak T)/intensity (peak C)	Ratio indicating shift from tryptophan-like to humic-like DOC
SUVA	Absorbance at 254 nm/DOC	DOC quality as indicator of carbon aromaticity

dataset (Table A1, Fig. A3, ESI†). Eqn (2a) and (b) describe the underlying terms involved for calculating corrected values (fDOM$_{corr}$) from fDOM$_{meas}$ in two steps.

$$\text{fDOM}_{\text{corr\_temp}} = \text{fDOM}_{\text{meas}} + \rho \frac{(T_{\text{meas}} - 25)}{r_{\text{p}}(\text{FNU})} \qquad (2a)$$

$$\text{fDOM}_{\text{corr}} = \frac{\text{fDOM}_{\text{corr\_temp}}}{r_{\text{d}}(A_{254})} + \text{fDOM}_{\text{corr\_temp}} \qquad (2b)$$

where fDOM$_{corr\_temp}$ is the temperature and turbidity corrected fDOM, T_{meas} is the measured water temperature, ρ is the temperature-specific fluorescence coefficient, and r_{p} and r_{d} are instrument-specific correction functions for suspended particulates and dissolved substances (scattering and absorbance) both varying from 0 to 1. For details, readers are referred to Downing et al.[32] The temperature-specific fluorescence coefficient ρ was determined by linear regression of fluorescence intensities against temperature for two different temperatures (6 and 17 °C). Eqn (2a) relates fDOM$_{meas}$ to a reference temperature of 25 °C.

The correction function for turbidity is based on the relationship between turbidity and fluorescence observations at fixed temperature and DOC concentration (calibration dataset).

In this study, the IFE correction factor r_{d} (eqn (2a) and (b)) was obtained by following an absorbance-based approach[50] described in detail in Kothawala et al.[51] This method is advantageous as no further measurements are necessary. The correction is based on available data (dilution experiments, calibration dataset) using the absorbance at the same wavelength pair as excitation and emission of the fDOM sensor. Thus, correction for IFE was performed according to Kothawala et al.:[51]

$$F_{\lambda_{\text{Ex}}, \lambda_{\text{Em}}}^{\text{IFE\_Corr}} = F_{\lambda_{\text{Ex}}, \lambda_{\text{Em}}}^{\text{Obs}} 10^{0.5\left(A_{\lambda_{\text{Ex}}} + A_{\lambda_{\text{Em}}}\right)} \qquad (3)$$

where F is the fluorescence signals of the excitation and the emission wavelength λ, A is the respective Abs$_{254}$, and superscripts Corr and Obs refer to corrected and observed signal, respectively (the observed signal in our case is the temperature- and turbidity-corrected fDOM time series, i.e. fDOM$_{corr\_temp}$).

Subsequently, for both r_{d} and r_{p}, the fluorescence data were translated into fDOM attenuation [%] (i.e. percentage difference between pre- and post-correction fDOM is reported) and expressed as a function of Abs$_{254}$ or turbidity (r_{d}, r_{p} in eqn (2a) and (b)). For instance, an attenuation of 20% translates into a r_{d} of 0.8, i.e. no attenuation is expressed by a r_{d} of 1. The fDOM$_{corr}$ was calculated according to eqn (2b).

Finally, a DOC model was obtained by linear regression between fDOM$_{corr}$ and observed DOC concentrations. The DOC concentrations estimated from the fDOM$_{corr}$ measurements are referred to as DOC$_{fDOM}$.

2.6.4. In situ absorbance corrections and DOC estimation. To account for baseline shifts in the spectrolyser dataset, the mean absorbance from 700 to 732.5 nm was subtracted from the full spectrum. The baseline-corrected absorbance data was used to predict DOC concentrations using a partial least square (PLS) regression model. The values from the 214 wavelengths were all used as the explanatory variables (predictors) in the model. In a PLS, $R^{2}Y$ indicates how much variation in the response variables is explained by the predictors, Q^{2} indicates the predictive ability of the model (derived by subtracting the ratio between predicted residual sum of squares and sum of squares from one), and the variable important for the projection (VIP) indicates the relative importance of the predictors (VIP > 1 indicate important variables).[52] PLS analyses are appropriate in the case of overfitting (i.e. number of predictor variables is higher than the number of observations) and strong collinearity between predictors.[53] A model with 2 latent variables was established and statistical coefficients were used to analyse the model's performance. The DOC concentrations estimated from the spectrolyser measurements are referred to as DOC$_{AbsMod}$.

2.6.5. Statistical analyses. The strength of correlations between estimated and observed DOC concentrations was assessed using the coefficient of determination R^{2} and the root mean square error RMSE.

The significance of trends of fluorescence indices based on a significance level of 0.05 was evaluated using the Mann–Kendall test,[54] which is a non-parametric test known for giving robust results for evaluating temporal trends in water quality-related parameters.[55,56]

3. Results

3.1. DOC concentrations and character measured in the laboratory

Dry conditions were present for most of the study period, with 304 mm of precipitation from May to September producing an average flow of 1.6 m^3 s^{-1}. The precedent snow melt episode led to a maximum discharge of 11.6 m^3 s^{-1} on March 23rd, whereas a rain storm at the end of October (28th) produced a maximum discharge of 16.1 m^3 s^{-1} (Fig. 2). These
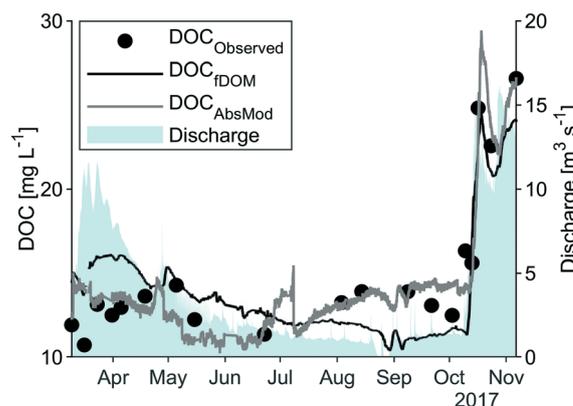

Fig. 2 Time series (March to November 2017) of discharge measurements, DOC concentrations of grab samples analysed in the laboratory (DOC$_{Observed}$) and estimated DOC concentrations based on the fDOM and spectrolyser measurements in the Fyris river.

This journal is © The Royal Society of Chemistry 2020

Environ. Sci.: Water Res. Technol., 2020, **6**, 2891–2901 | **2895**

values are comparably small in relation to long-term average flow data of 13.8 m^3 s^{-1}. DOC concentrations followed the discharge pattern (Fig. 2) with highest concentrations in October (up to 26.5 mg L^{-1}) and stable conditions during the summer period (at around 13.5 mg L^{-1}).

Optical indices derived from laboratory measurements are presented in Table 2. HIX was the first to reach near-maximum values towards the end of the discharge snow melt peak, directly followed by FI and SUVA. Simultaneously, the T/C ratio and $\beta:\alpha$ decreased to (near-) minimum values as they are inversely correlated to the aforementioned indices. During the low-flow and low-precipitation months of May to September, significant negative trends (Mann–Kendall test at $\alpha = 0.05$) were observed for SUVA ($p = 0.0163$, slope = -0.004 d^{-1}) and HIX ($p = 0.0069$, slope = -0.0001 d^{-1}) and a positive trend for $\beta:\alpha$ ($p = 0.0027$, slope = 0.0006 d^{-1}). During the storm in mid-October, HIX, FI, SUVA and T/C peak changed concurrently to the DOC concentration and reached extreme values (either maximum or minimum depending on the index).

Calculated HS concentrations ranged from 6.7 to 18.2 mg L^{-1} with a mean of 9.2 mg L^{-1}. The relative proportion of HS to DOC decreased from *ca.* 80% during the spring flood period to *ca.* 50% in September, and then rapidly increased following the autumn discharge peak to *ca.* 70%.

3.2. Comparisons of observed and estimated DOC concentrations from *in situ* measurements

High-frequency measurements were collected from March to November with only short interruptions. Power outages and technical problems (*e.g.* software issues) led to gaps in the spectrolyser time series during March and April. Generally, weather conditions were reflected by the high-frequency measurements with stable observations of turbidity, conductivity and temperature in the months May to September and extreme values of turbidity and fDOM$_{meas}$ in March and October. Systematic shifts in the data due to periodical manual cleaning were not apparent.

3.2.1. fDOM sensor. The instrument-specific correction functions were derived from the calibration data sets, which contained 57 data points mostly covering the data range of fDOM$_{meas}$ (68 to 138 QSU) and turbidity (22 to 47 FNU) measurements. The majority (61.2%) of fDOM$_{meas}$ were within this range, as well as most of the elevated turbidity values (at low turbidity levels, signals are less prone to particle influences). Based on the observed slopes of fDOM$_{meas}$ *versus* temperature, a coefficient of -0.012 °C^{-1} was derived. This corresponds to a decrease of 1.2% in the fDOM$_{meas}$ signal per 1 °C increase in water temperature. fDOM$_{corr}$ signal had lower variance than fDOM$_{meas}$ (Fig. A4, ESI†). The temperature correction led to a mean correction of 18% (ratio only temperature corrected fDOM$_{corr\_temp}$/ fDOM$_{meas}$) and was strongest in March when temperatures were lowest. Applying the turbidity correction increased fDOM$_{meas}$ during high turbidity events (*e.g.* see Fig. A4, ESI†: mid-March, mid-October). Multiplication with IFE correction function shifted the signal upwards.

As visible in Fig. A4, ESI†, fDOM$_{corr}$ compares to the pattern of laboratory DOC in spring and autumn, but in

Table 2 Optical indices, dissolved organic carbon (DOC) and humic substances (HS) concentrations, and fluorescent dissolved organic matter (fDOM) data during sampling events. The humification index (HIX), fluorescence index (FI) and freshness index ($\beta:\alpha$) were calculated from laboratory fluorescence measurements of grab samples from Storvad, as well as the specific ultraviolet absorbance (SUVA) from laboratory absorbance and DOC concentration measurements. All data, except for the corrected fDOM (fDOM$_{corr}$ EXO2), estimated DOC concentrations from the fDOM model (DOC$_{fDOM}$) and estimated DOC concentrations from the spectrolyser model (DOC$_{AbsMod}$), come from offline grab samples analysed in the laboratory

Date	HIX	FI	$\beta:\alpha$	SUVA	DOC [mg L^{-1}]	HS^a [mg L^{-1}]	HS/DOC	T/C	fDOM lab [QSU]	fDOM$_{corr}$ EXO2 [QSU]
Mar 09	0.94	1.50	0.57	3.34	11.9	8.7	0.73	0.26	169	146
Mar 16	0.92	1.51	0.56	3.35	10.7	8.0	0.75	0.28	156	136
Mar 23	0.94	1.48	0.54	3.35	13.1	9.9	0.76	0.21	185	170
Mar 31	0.93	1.47	0.54	3.85	12.5	10.3	0.82	0.22	183	171
Apr 05	0.94	1.48	0.55	3.58	13.0	10.0	0.78	0.22	180	171
Apr 18	0.94	1.45	0.56	3.16	13.6	9.4	0.69	0.27	160	147
May 05	0.93	1.46	0.55	3.24	14.3	9.5	0.66	0.26	157	147
May 15	0.93	1.45	0.56	3.14	12.2	8.5	0.70	0.30	141	132
Jun 22	0.91	1.06	0.59	2.96	11.4	7.6	0.67	0.41	125	116
Aug 03	0.91	1.47	0.61	2.78	13.2	8.2	0.62	0.45	126	109
Aug 14	0.91	1.50	0.61	2.52	13.9	7.8	0.56	0.53	109	106
Sep 08	0.90	1.50	0.64	2.28	13.9	7.2	0.52	0.46	111	93
Sep 21	0.89	1.48	0.64	2.60	13.1	7.6	0.58	0.48	112	97
Oct 02	0.90	1.48	0.63	2.70	12.5	7.6	0.61	0.43	118	104
Oct 09	0.90	1.50	0.63	2.09	16.3	7.6	0.47	0.46	117	100
Oct 13	0.93	1.54	0.59	3.23	15.6	10.8	0.69	0.25	187	181
Oct 16	0.94	1.50	0.54	3.35	24.8	17.1	0.69	0.22	301	272
Oct 23	0.94	1.50	0.53	3.39	22.6	15.8	0.70	0.21	246	248
Nov 06	0.95	1.51	0.51	3.34	26.6	18.2	0.68	0.18	289	293
R^2 DOC$_{fDOM}$	0.69	0.05	0.65	0.41	0.71	0.96	0.24	0.63	0.98	1.0
R^2 DOC$_{AbsMod}$	0.22	0.08	0.22	0.05	0.92	0.86	0.00	0.18	0.71	0.74

^{a} Calculated from eqn (1).

2896 | *Environ. Sci.: Water Res. Technol.*, 2020, **6**, 2891–2901

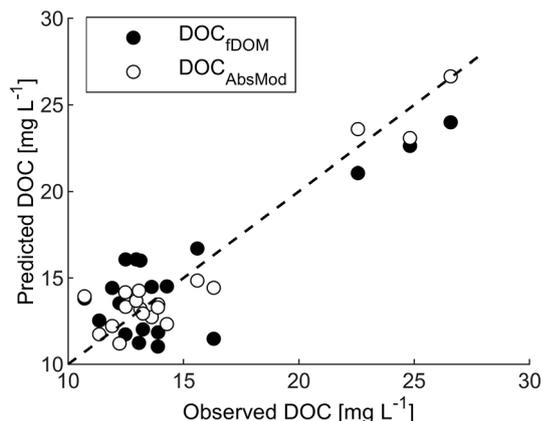This journal is © The Royal Society of Chemistry 2020

Fig. 3 Predicted *versus* measured DOC for the fDOM and spectrolyser. Dashed line represents the 1 : 1 line.

contrast to the stable DOC observations from May to September, it decreased steadily (from 160 QSU to 83 QSU) leading to deviations between the two signals. Correlation between measured DOC and the fDOM$_{corr}$ resulted in a R^2 of 0.71 and a RMSE of 2.5 mg L^{-1} (Fig. 3 and Table 2).

Despite the observed trends for the summer period in HIX, SUVA and $\beta : \alpha$, none of the indices described well the overall variation in the fDOM$_{corr}$ signal. HIX ($R^2 = 0.69$) and $\beta : \alpha$ ($R^2 = 0.65$) correlated better with fDOM$_{corr}$ than SUVA ($R^2 = 0.41$) and FI ($R^2 \leq 0.1$). The fDOM$_{corr}$ deviations were best-explained by the HS concentrations ($R^2 = 0.96$).

3.2.2. Absorbance sensor. A 2-component PLS model (Table A2, ESI†) was established based on the measured absorbance spectra, which explained 92% of the variation in DOC concentrations (*i.e.* $R^2Y = 0.92$) with a high predictive ability ($Q^2 = 0.85$). Thus, the estimated DOC based on the model correlated well with the measured DOC ($R^2 = 0.92$, RMSE = 1.3 mg L^{-1}, Fig. 3) and captured well the DOC dynamics (Fig. 2). Most of the 214 wavelengths were important predictors in the PLS model (VIP > 1), except for the higher wavelengths (larger than *ca.* 530 nm) (Fig. A5, ESI†). The estimated DOC from the spectrolyser did not significantly correlate with any of the optical indices (HIX, FI,
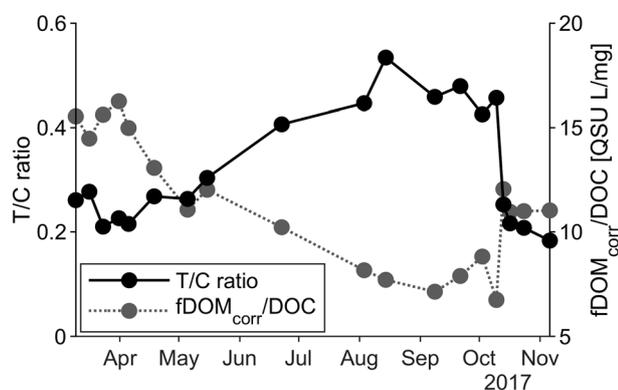
$\beta : \alpha$ and SUVA) during the sampling events (all $R^2 < 0.25$, $p > 0.01$, Table 2), but a significant correlation with HS was apparent ($R^2 = 0.86$, $p < 0.001$).

4. Discussion

4.1. Sensor evaluation – comparison of DOC estimations

pt?>Both sensors delivered estimates of DOC concentration in the form of high-frequency time series, however, their success at predicting laboratory-based DOC measurement differed. Although both instruments required data post-processing, this was most onerous for the fDOM sensor, which required compensation for temperature, turbidity and IFE, including dedicated experiments to establish sensor- and site-specific corrections. Under the conditions of our study, the spectrolyser resulted in better estimates of DOC concentration than the fDOM sensor. The RMSE for the fDOM sensor estimation (2.5 mg L^{-1}) was greater than that for the spectrolyser (1.3 mg L^{-1}). The absorbance-based DOC model was satisfactory, confirming the suitability of the modelling approach and the stability of the spectrolyser over time. PLS regression from absorbance data has successfully been used previously for calculating DOC concentrations.[57,58] On the other hand, in contrast to earlier studies that reported online fDOM to be a reliable proxy for DOC concentration (*e.g.* $R^2 = 0.79$,[59] $R^2 = 0.96$,[60] $R^2 = 0.93$ and 0.85[17]), we observed a period of relatively poor prediction between May and September.

Ruling out errors in setup and data treatment is essential before attempting to explain the differences between observed and estimated DOC by natural processes. Differences between the predictions by the two sensors cannot be explained by instrument setup since flow cell construction and installation were similar for both sensors (Fig. A1, ESI†). Another fDOM sensor installed 9 km downstream at Bärbyleden (Fig. 1), recorded similar fDOM as the one analysed in depth here, as demonstrated by linear correlation with a R^2 of 0.99 between the fDOM$_{meas}$ datasets of the two sensors (data not shown). The fDOM data corrections employed here included a combination of instrument- and site-specific factors, which complicates direct comparisons with other studies that used slightly different approaches in settings with different specific characteristics. However, molecular fluorescence of humic-like organic matter usually drops about 1% °C^{-1} increase in temperature[31,61] and our site-specific temperature correction factor of −0.009 °C^{-1} matches this and other published values.[34,62] Downing *et al.*[32] reported that about 10 to 19% of the fDOM signal was attenuated at a turbidity level of 50 FNU. Our results similarly showed an attenuation of 15% at 50 FNU. Downing *et al.*[32] also reported that correction of the IFE at an absorbance of 0.5 at 254 nm led to about 14 to 28% attenuation. Our correction resulted in an attenuation of 14% at this absorbance. Finally, comparing the field fDOM$_{corr}$ signal with laboratory fDOM measurements (fDOM lab) from grab samples revealed that, after normalization, the observed dynamics in these two signals were almost identical ($R^2 = 0.95$).

Fig. 4 Time series (March to November 2017) of the ratio between the peaks T and C and fDOM$_{corr}$/DOC ratio.

This journal is © The Royal Society of Chemistry 2020

Environ. Sci.: Water Res. Technol., 2020, **6**, 2891–2901 | **2897**

Our results do indicate that the fDOM$_{corr}$ signal was influenced by changes in DOC character in Fyrisån between March and September. As DOC quantity was stable during long periods of the late spring and summer, we are confident that the measured spectroscopic properties reflected changes in DOC character. The observed trends of HIX, SUVA and $\beta:\alpha$ from April to September indicate a shift in the DOC quality. During low-flow summer conditions, riverine DOC is composed of less-humified material with a larger contribution of more freshly produced DOC (lower HIX, higher $\beta:\alpha$) compared to high-flow conditions. The aromaticity (SUVA) decreased simultaneously and a shift occurred from humic-like (peak C) to protein-like (peak T) organic matter. Underlying reasons are a combination of several processes taking place in both the soil and the water column. On the one hand, during the summer months, low discharge and longer residence times trigger microbial in-stream processes that can lead to the production of microbially-derived DOC. Elevated temperatures enhance microbial activity and the photosynthetic activity of diatoms; evidence of the latter is seen in the decreasing silica concentrations in nearby Klastorp (Fig. A2, ESI†). Similar in-stream processes affecting DOC are typically observed in Mediterranean catchments where dry summer conditions occur frequently.[63] On the other hand, a change of the DOC source from the catchment can be considered likely. Our records from the monitoring station at Klastorp indicate that during high discharge, and thus during periods with elevated groundwater tables, absorbance, filtered iron and, consequently, SUVA are increased (Fig. A2 and A6, ESI†), which can be explained by the mobilization of water from shallow riparian soil levels. This is in accordance with the dominant source layer concept.[64] At low discharge, groundwater tables are low leading to lateral water inputs from deeper, mineral-like soil layers, which inherit DOC that is less aromatic, more microbially derived, and more recently produced than that from shallow organic riparian layers.[20] At deeper soil layers, the character of DOC changes due to the selective removal of terrestrial carbon during soil passage, whereby DOC attaches to mineral surfaces or flocculates with iron or aluminium hydroxides.[51]

From March to September, we observed lower concentrations of HS and fresher DOC (Table 2), probably due to release of degraded organic matter of the riparian vegetation and from high in-stream processing of fresh organic matter. Changes in the ratio of fDOM$_{corr}$ per DOC can be a consequence of these processes (Fig. 4). Furthermore, the pattern of the T/C ratio supported the DOC compositional variations. As the signal decreased during the summer months, a shift from the humic-like to the tryptophan-like peak occurred, indicating a shift from allochthonous terrestrial organic matter to autochthonous material, hence greater degree of microbial activity. Monitoring data from the Klastorp site support this conclusion, highlighting the typical annual pattern of high

flow, high silica under cold periods and low flow, warm temperature and biological in-stream processing of silica in summer (Fig. A2, ESI†).

We hypothesize that earlier observed good fits between fDOM and DOC were established in surface waters with a smaller fraction of agricultural land use and/or less temporally-variable DOC character, e.g. in lakes[32,60,65] that represent more stable environments than our river water. As such, care needs to be taken when using a fDOM sensor for estimating DOC concentrations in lotic waters.

4.2. Application in drinking water treatment

Next to practicalities such as acquisition cost, maintenance and power requirements, the best choice of sensor depends on the monitoring aim and the catchment under investigation. The required accuracy of DOC concentration estimations differs depending on the application of the sensors. For illustration, if during the drinking water production process 3 to 4 mg L^{-1} were removed, then a DOC estimation error of 1.5 mg L^{-1} would not be satisfactory. However, for deciding on temporary interruptions of the water intake due to a high concentration event, it might still fulfil its purpose. For drinking water applications, the fDOM sensor might suffice if the main objective is to adjust chemical dose for coagulation processes. The HS, representing the organic matter fraction that can be removed by flocculation,[66] showed here a very good correlation with the fDOM$_{corr}$ (R^2 = 0.96). However, complex site- and instrument-specific corrections need to be applied to the data recorded by the fDOM sensor.

Grab sampling is also needed in order to maintain the sensors as well as to improve the correction functions. If measurement of several parameters is intended, it might be justified to invest in a full-spectrum sensor and to calibrate it to parameters of interest (e.g. HS fraction, DOC, turbidity). The spectrolyser would be a more reliable choice for predicting DOC, especially in flashy catchments. This study indicates that greater precision in DOC concentration estimates can be achieved if information from a broad range of wavelengths is available as compared to a single excitation sensor.

Sensors offer well-known advantages over intermittent samples, especially the possibility of reacting immediately to changes in the raw water quality, allowing for real-time adjustment of processes such as MAR. Grab samples are prone to miss certain events leading to false assumptions about DOC dynamics, as exemplified here by comparing linearly interpolating DOC concentrations of the grab samples with the estimated DOC concentrations from the spectrolyser, where systematic differences of up to ±4 mg L^{-1} are present at several periods of days (Fig. A7, ESI†). At drinking water facilities, tracking and responding to changes in DOC character can reduce costs of chemicals and increase membrane lifetimes by reducing backwashing frequency. Once reliable routines for treating sensor data are developed, personnel costs will diminish due to a reduced need for grab samples and laboratory analyses.

2898 | *Environ. Sci.: Water Res. Technol.*, 2020, **6**, 2891–2901

This journal is © The Royal Society of Chemistry 2020

5. Conclusions

In this study, a fluorescence- and an absorbance-based sensor were evaluated in relation to their accuracy for estimating DOC concentrations and in their applicability for drinking water production. Both sensors were found to be suitable supportive tools for MAR depending on the water quality parameters of greatest interest at the treatment plant.

Optical indices derived from grab samples indicated temporal changes in the DOC character throughout the measuring period in this mixed forested and agricultural landscape. These changes impacted the accuracy of the compared sensors differently. The EXO2 fDOM sensor provided periodically inaccurate predictions of DOC; however, if the objective is to monitor the easily-removed DOC fraction (*i.e.* HS), then the fDOM sensor is a suitable solution assuming that a convenient post-processing data pipeline can be developed. Further confirmation of the stability of the fDOM–HS relationship is needed. In contrast, the multiple-wavelength model based on spectrolyser absorbance spectra reliably compensated for changes in DOC composition. Expanding the dataset to measure more data under extreme conditions will improve the prediction of the full range of DOC concentrations.

Conflicts of interest

There are no conflicts to declare.

Acknowledgements

References

1 B. Bates, Z. W. Kundzewicz, S. Wu and J. Palutikof, *Climate Change and Water. Technical Paper of the Intergovernmental Panel on Climate Change*, IPCC Secr., Geneva, 2008, p. 210.

2 SOU 2007:60, Final report from the Swedish Commission on Climate and Vulnerability, in *Sweden facing climate change – threats and opportunities*, Swedish Government Official Reports, Stockholm, 2007.

3 H. A. De Wit, S. Valinia, G. A. Weyhenmeyer, M. N. Futter, P. Kortelainen, K. Austnes, D. O. Hessen, A. Räike, H. Laudon and J. Vuorenmaa, Current Browning of Surface Waters Will Be Further Promoted by Wetter Climate, *Environ. Sci. Technol. Lett.*, 2016, **3**, 430–435, DOI: 10.1021/acs.estlett.6b00396.

4 C. D. Evans, T. G. Jones, A. Burden, N. Ostle, P. Zieliński, M. D. A. Cooper, M. Peacock, J. M. Clark, F. Oulehle, D. Cooper and C. Freeman, Acidity controls on dissolved organic carbon mobility in organic soils, *Glob. Change Biol.*, 2012, **18**, 3317–3331, DOI: 10.1111/j.1365-2486.2012.02794.x.

5 N. Roulet and T. R. Moore, Browning the waters, *Nature*, 2006, **444**, 283–284, DOI: 10.1038/444283a.

6 N. Her, G. Amy, J. Chung, J. Yoon and Y. Yoon, Characterizing dissolved organic matter and evaluating associated nanofiltration membrane fouling, *Chemosphere*, 2008, **70**, 495–502, DOI: 10.1016/j.chemosphere.2007.06.025.

7 M.-G. Kang, Y.-H. Ku, Y.-K. Cho and M.-J. Yu, Variation of dissolved organic matter and microbial regrowth potential through drinking water treatment processes, *Water Sci. Technol.: Water Supply*, 2006, **6**, 57–66, DOI: 10.2166/ws.2006.904.

8 M. J. Nieuwenhuijsen, J. Grellier, R. Smith, N. Iszatt, J. Bennett, N. Best and M. Toledano, The epidemiology and possible mechanisms of disinfection by-products in drinking water, *Philos. Trans. R. Soc., A*, 2009, **367**, 4043–4076, DOI: 10.1098/rsta.2009.0116.

9 S. Richardson, M. Plewa, E. Wagner, R. Schoeny and D. Demarini, Occurrence, genotoxicity, and carcinogenicity of regulated and emerging disinfection by-products in drinking water: A review and roadmap for research, *Mutat. Res.*, 2007, **636**, 178–242, DOI: 10.1016/j.mrrev.2007.09.001.

10 L. E. Anderson, W. H. Krkošek, A. K. Stoddart, B. F. Trueman and G. A. Gagnon, Lake Recovery Through Reduced Sulfate Deposition: A New Paradigm for Drinking Water Treatment, *Environ. Sci. Technol.*, 2017, **51**, 1414–1422, DOI: 10.1021/acs.est.6b04889.

11 A. Keucken, G. Heinicke, K. Persson and S. Köhler, Combined Coagulation and Ultrafiltration Process to Counteract Increasing NOM in Brown Surface Water, *Water*, 2017, **9**, 697, DOI: 10.3390/w9090697.

12 N. M. Kortelainen and J. A. Karhu, Tracing the decomposition of dissolved organic carbon in artificial groundwater recharge using carbon isotope ratios, *Appl. Geochem.*, 2006, **21**, 547–562, DOI: 10.1016/j.apgeochem.2006.01.004.

13 P. Baveye, P. Vandevivere, B. L. Hoyle, P. C. DeLeo and D. Sanchez De Lozada, Environmental impact and mechanisms of the biological clogging of saturated soils and aquifer materials, *Crit. Rev. Environ. Sci. Technol.*, 1998, **28**, 123–191, DOI: 10.1080/10643389891254197.

14 K. H. Knorr, DOC-dynamics in a small headwater catchment as driven by redox fluctuations and hydrological flow paths – Are DOC exports mediated by iron reduction/oxidation cycles?, *Biogeosciences*, 2013, **10**, 891–904, DOI: 10.5194/bg-10-891-2013.

15 E. E. Lavonen, D. N. Kothawala, L. J. Tranvik, M. Gonsior, P. Schmitt-Kopplin and S. J. Köhler, Tracking changes in the optical properties and molecular composition of dissolved organic matter during drinking water production, *Water Res.*, 2015, **85**, 286–294, DOI: 10.1016/j.watres.2015.08.024.

This journal is © The Royal Society of Chemistry 2020

Environ. Sci.: Water Res. Technol., 2020, **6**, 2891–2901 | **2899**

16 D. M. McKnight, E. W. Boyer, P. K. Westerhoff, P. T. Doran, T. Kulbe and D. T. Andersen, Spectrofluorometric characterization of dissolved organic matter for indication of precursor organic material and aromaticity, *Limnol. Oceanogr.*, 2001, **46**, 38–48, DOI: 10.4319/lo.2001.46.1.0038.

17 Y. Shutova, A. Baker, J. Bridgemann and R. K. Henderson, On-line monitoring of organic matter concentrations and character in drinking water treatment systems using fluorescence spectroscoy, *Environ. Sci.: Water Res. Technol.*, 2016, **2**, 749–760.

18 J. Wasswa, N. Mladenov and W. Pearce, Assessing the potential of fluorescence spectroscopy to monitor contaminants in source waters and water reuse systems, *Environ. Sci.: Water Res. Technol.*, 2019, **5**(2), 370–382.

19 J. L. Weishaar, G. R. Aiken, B. A. Bergamaschi, M. S. Fram, R. Fujii and K. Mopper, Evaluation of specific ultraviolet absorbance as an indicator of the chemical composition and reactivity of dissolved organic carbon, *Environ. Sci. Technol.*, 2003, **37**, 4702–4708, DOI: 10.1021/es030360x.

20 J. L. J. Ledesma, D. N. Kothawala, P. Bastviken, S. Maehder, T. Grabs and M. N. Futter, Stream Dissolved Organic Matter Composition Reflects the Riparian Zone, Not Upslope Soils in Boreal Forest Headwaters, *Water Resour. Res.*, 2018, **54**, 3896–3912, DOI: 10.1029/2017WR021793.

21 K. R. Murphy, C. A. Stedmon, T. D. Waite and G. M. Ruiz, Distinguishing between terrestrial and autochthonous organic matter sources in marine environments using fluorescence spectroscopy, *Mar. Chem.*, 2008, **108**, 40–58, DOI: 10.1016/j.marchem.2007.10.003.

22 C. A. Stedmon, S. Markager and R. Bro, Tracing dissolved organic matter in aquatic environments using a new approach to fluorescence spectroscopy, *Mar. Chem.*, 2003, **82**, 239–254, DOI: 10.1016/S0304-4203(03)00072-0.

23 A. Stubbins, J. F. Lapierre, M. Berggren, Y. T. Prairie, T. Dittmar and P. A. Del Giorgio, What's in an EEM? Molecular signatures associated with dissolved organic fluorescence in boreal Canada, *Environ. Sci. Technol.*, 2014, **48**, 10598–10606, DOI: 10.1021/es502086e.

24 P. J. Hernes, B. A. Bergamaschi, R. S. Eckard and R. G. M. Spencer, Fluorescence-based proxies for lignin in freshwater dissolved organic matter, *J. Geophys. Res.: Space Phys.*, 2009, **114**, G00F03, DOI: 10.1029/2009JG000938.

25 S. A. Huber, A. Balz, M. Abert and W. Pronk, Characterisation of aquatic humic and non-humic matter with size-exclusion chromatography – organic carbon detection – organic nitrogen detection (LC-OCD-OND), *Water Res.*, 2011, **45**, 879–885, DOI: 10.1016/j.watres.2010.09.023.

26 P. Bose and D. A. Reckhow, The effect of ozonation on natural organic matter removal by alum coagulation, *Water Res.*, 2007, **41**, 1516–1524, DOI: 10.1016/j.watres.2006.12.027.

27 M. Edwards, Predicting DOC removal during enhanced coagulation, *J. - Am. Water Works Assoc.*, 1997, **89**, 78–89, DOI: 10.1002/j.1551-8833.1997.tb08229.x.

28 S. J. Köhler, E. Lavonen, A. Keucken, P. Schmitt-Kopplin, T. Spanjer and K. Persson, Upgrading coagulation with hollow-fibre nanofiltration for improved organic matter removal during surface water treatment, *Water Res.*, 2016, **89**, 232–240, DOI: 10.1016/j.watres.2015.11.048.

29 C. R. O'Melia, W. C. Becker and K. K. Au, Removal of humic substances by coagulation, *Water Sci. Technol.*, 1999, **40**, 47–54, DOI: 10.1016/S0273-1223(99)00639-3.

30 H. Laudon, M. Berggren, A. Ågren, I. Buffam, K. Bishop, T. Grabs, M. Jansson and S. J. Köhler, Patterns and Dynamics of Dissolved Organic Carbon (DOC) in Boreal Streams: The Role of Processes, Connectivity, and Scaling, *Ecosystems*, 2011, **14**, 880–893, DOI: 10.1007/s10021-011-9452-8.

31 A. Baker, Thermal fluorescence quenching properties of dissolved organic matter, *Water Res.*, 2005, **39**, 4405–4412, DOI: 10.1016/j.watres.2005.08.023.

32 B. D. Downing, B. A. Pellerin, B. A. Bergamaschi, J. F. Saraceno and T. E. C. Kraus, Seeing the light: The effects of particles, dissolved materials, and temperature on in situ measurements of DOM fluorescence in rivers and streams, *Limnol. Oceanogr.: Methods*, 2012, **10**, 767–775, DOI: 10.4319/lom.2012.10.767.

33 J. F. Saraceno, J. B. Shanley, B. D. Downing and B. A. Pellerin, Clearing the waters : Evaluating the need for site-specific field fluorescence corrections based on turbidity measurements, *Limnol. Oceanogr.: Methods*, 2017, **15**, 408–416, DOI: 10.1002/lom3.10175.

34 C. J. Watras, P. C. Hanson, T. L. Stacy, K. M. Morrison, J. Mather, Y.-H. Hu and P. Milewski, A temperature compensation method for CDOM fluorescence sensors in freshwater, *Limnol. Oceanogr.: Methods*, 2011, **9**, 296–301, DOI: 10.4319/lom.2011.9.296.

35 K. Khamis, J. P. R. Sorensen, C. Bradley, D. M. Hannah, D. J. Lapworth and R. Stevens, In situ tryptophan-like fluorometers: assessing turbidity and temperature effects for freshwater applications, *Environ. Sci.: Processes Impacts*, 2015, **17**, 740–752, DOI: 10.1039/c5em00030k.

36 G. de Oliveira, E. Bertone, R. Stewart, J. Awad, A. Holland, K. O'Halloran and S. Bird, Multi-Parameter Compensation Method for Accurate In Situ Fluorescent Dissolved Organic Matter Monitoring and Properties Characterization, *Water*, 2018, **10**, 1146, DOI: 10.3390/w10091146.

37 J. L. J. Ledesma, S. J. Köhler and M. N. Futter, Long-term dynamics of dissolved organic carbon: Implications for drinking water supply, *Sci. Total Environ.*, 2012, **432**, 1–11, DOI: 10.1016/j.scitotenv.2012.05.071.

38 L. Gottschalk, J. L. Jensen, D. Lundquist, R. Solantie and A. Tollan, Hydrologic Regions in the Nordic Countries, *Hydrol. Res.*, 1979, **10**, 273–286.

39 J. F. Exbrayat, N. R. Viney, J. Seibert, S. Wrede, H. G. Frede and L. Breuer, Ensemble modelling of nitrogen fluxes: Data fusion for a Swedish meso-scale catchment, *Hydrol. Earth Syst. Sci.*, 2010, **14**, 2383–2397, DOI: 10.5194/hess-14-2383-2010.

40 HORIBA Instruments Incorporated, *AquaLog Operational Manual., Rev. B*, 2012.

41 A. J. Lawaetz and C. A. Stedmon, Fluorescence Intensity Calibration Using the Raman Scatter Peak of Water, *Appl. Spectrosc.*, 2009, **63**, 936–940, DOI: 10.1366/000370209788964548.

42 YSI Incorporated, a Xylem brand, *EXO2: EXO User Manual ADVANCED WATER QUALITY MONITORING PLATFORM*, 2017.

43 s::can Messtechnik GmbH, *S::can spectrometer probe: Manual s::can spectrometer probe*, 2007.

44 J. Fölster, R. K. Johnson, M. N. Futter and A. Wilander, The Swedish monitoring of surface waters: 50 years of adaptive monitoring, *Ambio*, 2014, **43**, 3–18, DOI: 10.1007/s13280-014-0558-z.

45 T. Ohno, Fluorescence inner-filtering correction for determining the humification index of dissolved organic matter, *Environ. Sci. Technol.*, 2002, **36**, 742–746, DOI: 10.1021/es0155276.

46 R. M. Cory and D. M. McKnight, Fluorescence Spectroscopy Reveals Ubiquitous Presence of Oxidized and Reduced Quinones in Dissolved Organic Matter, *Environ. Sci. Technol.*, 2005, **39**, 8142–8149, DOI: 10.1021/es0506962.

47 E. Parlanti, K. Wörz, L. Geoffroy and M. Lamotte, Dissolved organic matter fluorescence spectroscopy as a tool to estimate biological activity in a coastal zone submitted to anthropogenic inputs, *Org. Geochem.*, 2000, **31**, 1765–1781, DOI: 10.1016/S0146-6380(00)00124-8.

48 P. G. Coble, Characterization of marine and terrestrial DOM in seawater using excitation-emission matrix spectroscopy, *Mar. Chem.*, 1996, **51**, 325–346, DOI: 10.1016/0304-4203(95)00062-3.

49 Grundvattengruppen for Uppsala Vatten, Uppsala Vatten report, in *Funktionanalys Uppsalaåsen*, Uppsala, 2017.

50 J. R. Lakowicz, in *Principles of Fluorescence Spectroscopy*, ed. J. R. Lakowicz, Springer US, Boston, MA, 3rd edn, 2006, DOI: 10.1007/978-0-387-46312-4.

51 D. N. Kothawala, K. R. Murphy, C. A. Stedmon, G. A. Weyhenmeyer and L. J. Tranvik, Inner filter correction of dissolved organic matter fluorescence, *Limnol. Oceanogr.: Methods*, 2013, **11**, 616–630, DOI: 10.4319/lom.2013.11.616.

52 L. Eriksson, E. Johansson and S. Wold, *Introduction to Multi- and Megavariate Data Analysis Using Projection Methods (PCA & PLS)*, Umetrics AB, 1999.

53 L. M. Carrascal, I. Galván and O. Gordo, Partial least squares regression as an alternative to current regression methods used in ecology, *Oikos*, 2009, **118**, 681–690, DOI: 10.1111/j.1600-0706.2008.16881.x.

54 H. B. Mann, Nonparametric Tests Against Trend, *Econometrica*, 1945, **13**, 245–259, DOI: 10.2307/1907187.

55 C. D. Evans, D. T. Monteith and D. M. Cooper, Long-term increases in surface water dissolved organic carbon: Observations, possible causes and environmental impacts, *Environ. Pollut.*, 2005, **137**, 55–71, DOI: 10.1016/j.envpol.2004.12.031.

56 A. Prechtel, C. Alewell, M. Armbruster, J. Bittersohl, J. M. Cullen, C. D. Evans, R. Helliwell, J. Kopácek, A. Marchetto, E. Matzner, H. Meesenburg, F. Moldan, K. Moritz, J. Veselý and R. F. Wright, Response of sulphur dynamics in European catchments to decreasing sulphate deposition, *Hydrol. Earth Syst. Sci.*, 2001, **5**, 311–326, DOI: 10.5194/hess-5-311-2001.

57 J. R. Etheridge, F. Birgand, J. A. Osborne, C. L. Osburn, M. R. Burchell and J. Irving, Using in situ ultraviolet-visual spectroscopy to measure nitrogen, carbon, phosphorus, and suspended solids concentrations at a high frequency in a brackish tidal marsh, *Limnol. Oceanogr.: Methods*, 2014, **12**, 10–22, DOI: 10.4319/lom.2014.12.10.

58 M. C. H. Vaughan, W. B. Bowden, J. B. Shanley, A. Vermilyea, R. Sleeper, A. J. Gold, S. M. Pradhanang, S. P. Inamdar, D. F. Levia, A. S. Andres, F. Birgand and A. W. Schroth, High-frequency dissolved organic carbon and nitrate measurements reveal differences in storm hysteresis and loading in relation to land cover and seasonality, *Water Resour. Res.*, 2017, **53**, 5345–5363, DOI: 10.1002/2017WR020491.

59 J. T. Crawford, L. C. Loken, N. J. Casson, C. Smith, A. G. Stone and L. A. Winslow, High-speed limnology: Using advanced sensors to investigate spatial variability in biogeochemistry and hydrology, *Environ. Sci. Technol.*, 2015, **49**, 442–450, DOI: 10.1021/es504773x.

60 J. F. Saraceno, B. A. Pellerin, B. D. Downing, E. Boss, P. A. M. Bachand and B. A. Bergamaschi, High-frequency in situ optical measurements during a storm event: Assessing relationships between dissolved organic matter, sediment concentrations, and hydrologic processes, *J. Geophys. Res.: Biogeosci.*, 2009, **114**, 1–11, DOI: 10.1029/2009JG000989.

61 A. Vodacek and W. D. Philpot, Environmental effects on laser-induced fluorescence spectra of natural waters, *Remote Sens. Environ.*, 1987, **21**, 83–95, DOI: 10.1016/0034-4257(87)90008-3.

62 K. Khamis, C. Bradley, R. Stevens and D. M. Hannah, Continuous field estimation of dissolved organic carbon concentration and biochemical oxygen demand using dual-wavelength fluorescence, turbidity and temperature, *Hydrol. Processes*, 2017, 540–555, DOI: 10.1002/hyp.11040.

63 S. Bernal, A. Lupon, N. Catalán, S. Castelar and E. Martí, Decoupling of dissolved organic matter patterns between stream and riparian groundwater in a headwater forested catchment, *Hydrol. Earth Syst. Sci.*, 2018, **22**, 1897–1910, DOI: 10.5194/hess-22-1897-2018.

64 J. L. J. Ledesma, M. N. Futter, M. Blackburn, F. Lidman, T. Grabs, R. A. Sponseller, H. Laudon, K. H. Bishop and S. J. Köhler, Towards an Improved Conceptualization of Riparian Zones in Boreal Forest Headwaters, *Ecosystems*, 2018, **21**, 297–315, DOI: 10.1007/s10021-017-0149-5.

65 E. J. Lee, G. Y. Yoo, Y. Jeong, K. U. Kim, J. H. Park and N. H. Oh, Comparison of UV-VIS and FDOM sensors for in situ monitoring of stream DOC concentrations, *Biogeosciences*, 2015, **12**, 3109–3118, DOI: 10.5194/bg-12-3109-2015.

66 E. L. Sharp, S. A. Parsons and B. Jefferson, The impact of seasonal variations in DOC arising from a moorland peat catchment on coagulation with iron and aluminium salts, *Environ. Pollut.*, 2006, **140**, 436–443, DOI: 10.1016/j.envpol.2005.08.001.

This journal is © The Royal Society of Chemistry 2020

Environ. Sci.: Water Res. Technol., 2020, **6**, 2891–2901 | **2901**